3.2 Quasi-TEM Propagation Characteristics of Meandered CCS TLs and Conventional MSs

3.2.1 Analyses and Validity Checks of 2-D TLs

As discussed in Section 3.1, the CCS TL is a 2-D guiding structure since it is not uniform in the cross sections along the direction of propagation [See Fig. 3.1(b).]. Furthermore, the CCS TL may traverse in an arbitrarily meandered path. Full-wave resonance techniques for extracting the quasi-TEM propagation characteristics may not apply. What follows summarizes the procedure for extracting the effective complex propagation constant γ and the complex characteristic impedance Z_c from the theoretical and measured two-port scattering parameters. The effective complex propagation constant γ is denoted by $\gamma = j\beta + \alpha$, where β is the phase constant and α is the attenuation constant. Using the ABCD matrix representation of a two-port TL in terms of complex propagation constant γ and characteristic impedance Z_c, and the link between the ABCD matrix and the scattering parameters (S-parameters), one obtain the following equations [54],

$$e^{\gamma L} = \frac{1 - S_{11}^2 + S_{21}^2 + \sqrt{(1 + S_{11}^2 - S_{21}^2)^2 - (2S_{11})^2}}{2S_{21}}. \tag{3.5}$$

$$Z_c = Z_o \sqrt{\frac{(1+S_{11})^2 - S_{21}^2}{(1-S_{11})^2 - S_{21}^2}} \,. \tag{3.6}$$

Where Z_o is the referenced impedance, typically equal to 50 ohm; L is the total length of the meandered CCS TL, equal to P times the number of cells. Notably, the cyclically mapped phase of the scattering parameter (-180° to +180°) is converted to the true continuous radian phase during the extraction. The extracting formulas of the guiding properties for the generalized passive finite-length TL with different complex reference impedance (Z_1, Z_2 not equal to 50-Ω), and longer length (larger than quarter-wave-length) have been derived as in parts A to C of Appendix.

Throughout this dissertation, the full-wave simulator **Zeland** IE3D™ is employed for obtaining the two-port scattering parameters of the meandered TLs. Metal strip conductivity of 5.49×10^7 S/m and a thickness of 18 μm (approximately a 1/2-oz copper thickness), and the dielectric loss tangent of 0.002 are entered in the full-wave analyses.

Referring to the Fig. 3.2, the HMICs are made on a two-sided printed RO4003 circuit board of thickness (h) 0.203 mm and relative permittivity (ε_r) 3.38. For purpose of clarity, we present the propagation characteristics of quasi-TEM TLs by characterizing the TLs in terms of the SWF

(SWF= $\lambda_o / \lambda_g = \beta / k_o$ or the normalized phase constant) and the characteristic impedance ($Z_c(f)$), both of which are dispersive. The losses associated with the guiding structure are expressed by decibels/λ_g. All three parameters, namely, Z_c, SWF, and loss (decibels/λ_g), are readily derived from (3.5) and (3.6).

The validity checks of the above TL parameter-extraction procedure is conducted by comparing measured results and theoretical data using the same test circuit, which is shown in the inset of Fig. 3.3, i.e., a CCS TL meandered in the 5 × 4 2-D lattice. The CCS TL employs a unit cell of periodicity P equal to 450 μm, a top metal patch of dimensions $W_x = W_y = 300$ μm, a connecting arm of width S = 150 μm, and a square opening in the mesh ground plane of $W_{hx} = W_{hy} = 300$ μm. Fig. 3.3 plots both theoretical (in solid lines) and measured (in dotted solid lines) data, showing that 3.73% deviation in the normalized propagation constant and the theoretical values of the normalized attenuation constant (α/k_o) are very close to the lower bound of the measured data. The two sets of curves are in excellent agreement across the entire spectrum of interest from 0.5 GHz to 10 GHz. Thus, confidence in the theoretical extractions of propagation characteristics of the compacted meandered CCS TL is established. The discrepancy in complex γ could be caused by etching pattern, dimension errors and a small amount of internal multiple reflections since two subminiature A (SMA) connectors are soldered to the CCS TL in the test fixture for reliable

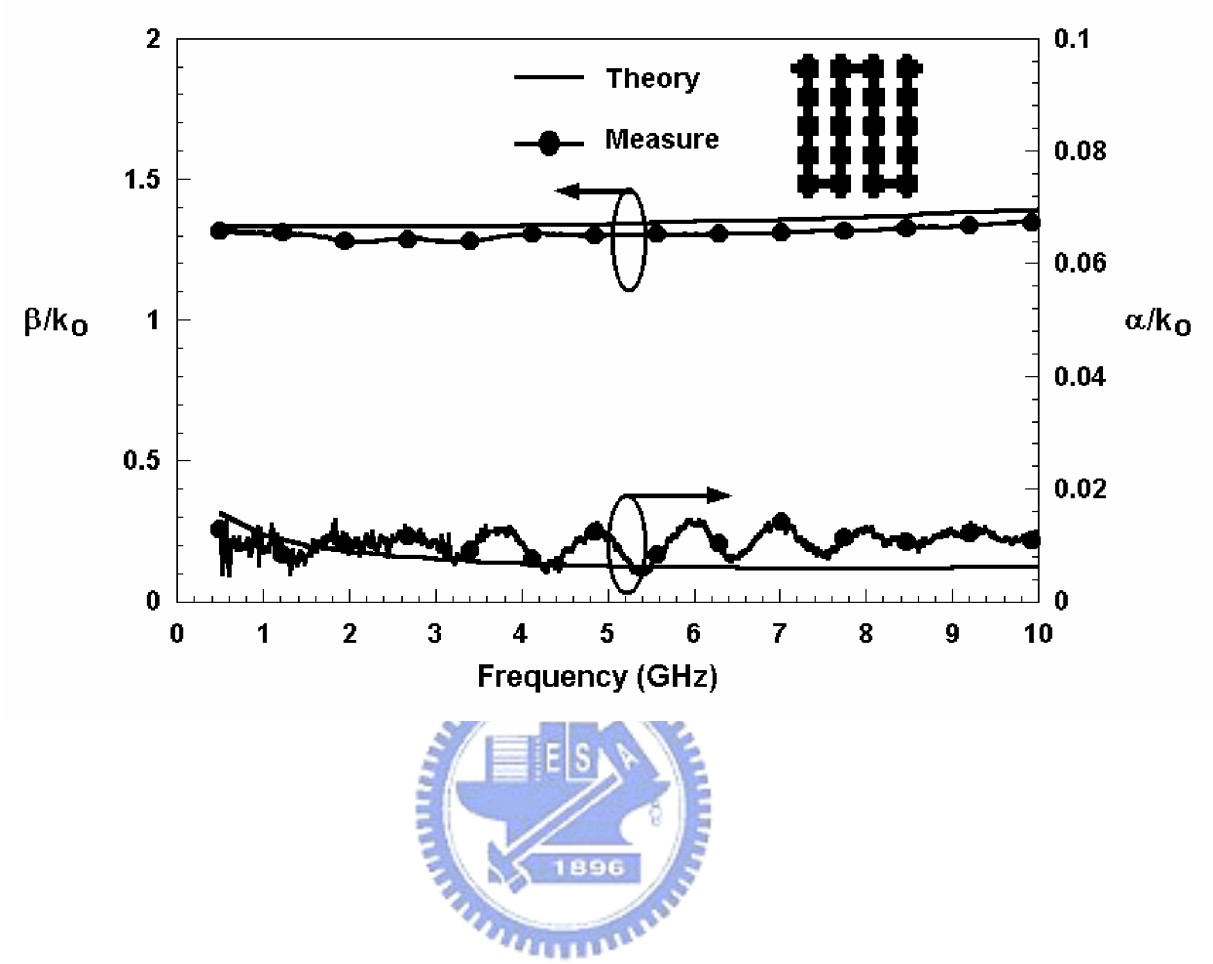

Fig. 3.3. Predicted and measured normalized propagation constants (phase constant β/k_o, attenuation constant α/k_o) versus frequency of the 70-Ω CCS TL (5×4 meander trace). Structural and material parameters are P = 450 μm, S = 150 μm, $W_x = W_y = W_{hx} = W_{hy}$ = 300 μm, L = 9020 μm, and h = 0.203 mm; the relative dielectric constant ε_r = 3.38 and t = 0.018 mm, and the conductivity of the metal is 5.49×10^7 S/m, as shown in Fig. 3.1 and Eq. (3.5).

S-parameters testing, and the residual reflections are still present after deembedding the test fixture.

Figure 3.4 compares the complex characteristic impedances obtained by extracting theoretical and measured scattering parameters for the same CCS TL reported in Fig. 3.3. The theoretical value of 72 Ω is slightly lower than that of measured data near 5.4 GHz. Across the 0.5-10-GHz band, the maximum (minimum) value of the real part of the characteristic impedance is 80(64) Ω, representing a deviation of +/- 11% from 72 Ω. The imaginary parts of both theoretical and measured complex characteristic impedances are nearly identical, except near the beginning and ending frequencies. The data shown in Fig. 3.4 also validate the theoretical predictions of the guiding characteristics of the compacted meandered CCS TL. The discrepancy in complex Z_c could be caused by etching pattern, dimension errors and an equivalent series inductor (L_s) and parallel capacitor (C_p) of coaxial-to-microstrip transition since two subminiature A (SMA) connectors are soldered to the CCS TL in the test fixture for reliable S-parameters testing, and the residual transitions are still present after deembedding the test fixture [2], [8].

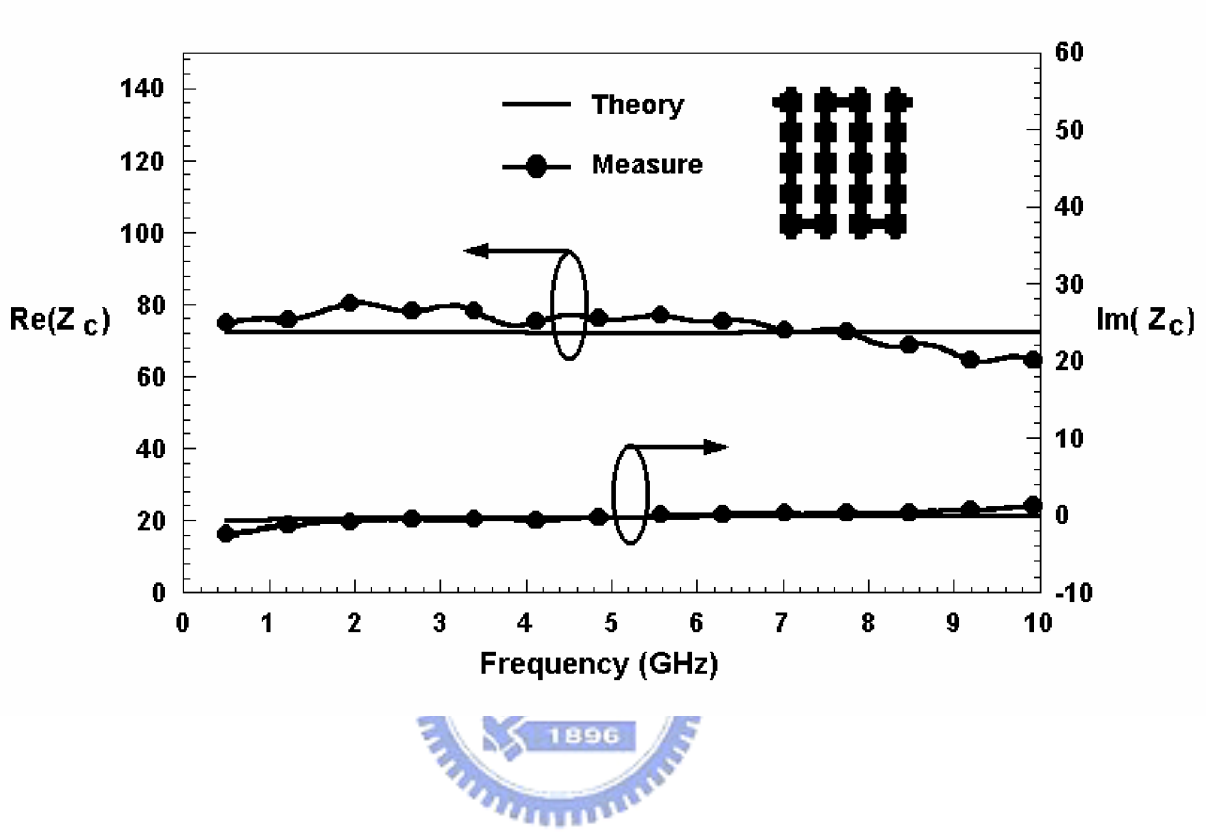

Fig. 3.4. Predicted and measured characteristic impedance (real part: $Re(Z_c)$, imaginary part: $Im(Z_c)$) versus frequency of the 70-Ω CCS TL (5×4 meander trace); structural and material parameters as in Fig. 3.3.

3.2.2 Comparative Studies of Propagation Characteristics of CCS TL Against MS in both Straight and Meandered Configurations

In the following, the propagation characteristics of a 2-D CCS TL as previously shown in the inset of Fig. 3.3 will be investigated by varying the planar structural parameters and comparing the extracted theoretical data of complex propagation constants and characteristic impedances against those of conventional MSs in both straight and meandered shapes. Assuming that all the guiding structures under investigations are made by the same process and design rules such that the minimum linewidth is 100 μm, the minimum line spacing is 100μm, and the material constants are the same as those applied for the CCS TL design reported in Figs. 3.3 and 3.4. The guiding properties, Re(Z_c) (real part Z_c), SWF, and Loss(dB/λ_g) of the 2-D CCS TL (5×4, meander trace) versus different values of patch width W (= W_x = W_y) under the conditions of various widths (S) of the connecting arm and changing sizes of etched ground planes W_h (= W_{hx} = W_{hy}) and the periodicity P of 450 and 225 μm at f_o = 5.4 GHz are displayed in Fig. 3.5(a)-(c), respectively.

This section investigates the guiding properties of a CCS TL realized by contemporary PCB process obeying design rules generally accepted by most manufacturers. Such investigations lead to the design of the compacted rat-race hybrid shown in Fig. 3.2. Useful design information and comparative studies

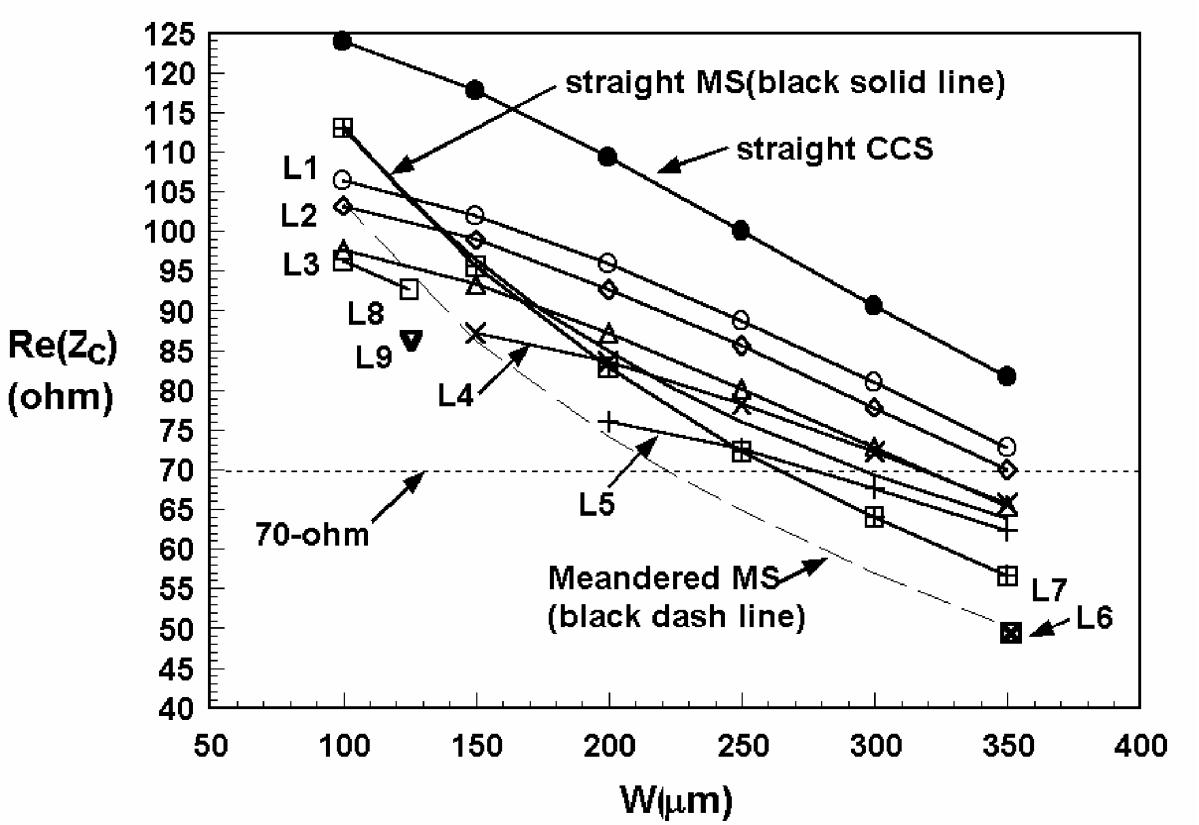

(a) The $Re(Z_c)$ vs. W

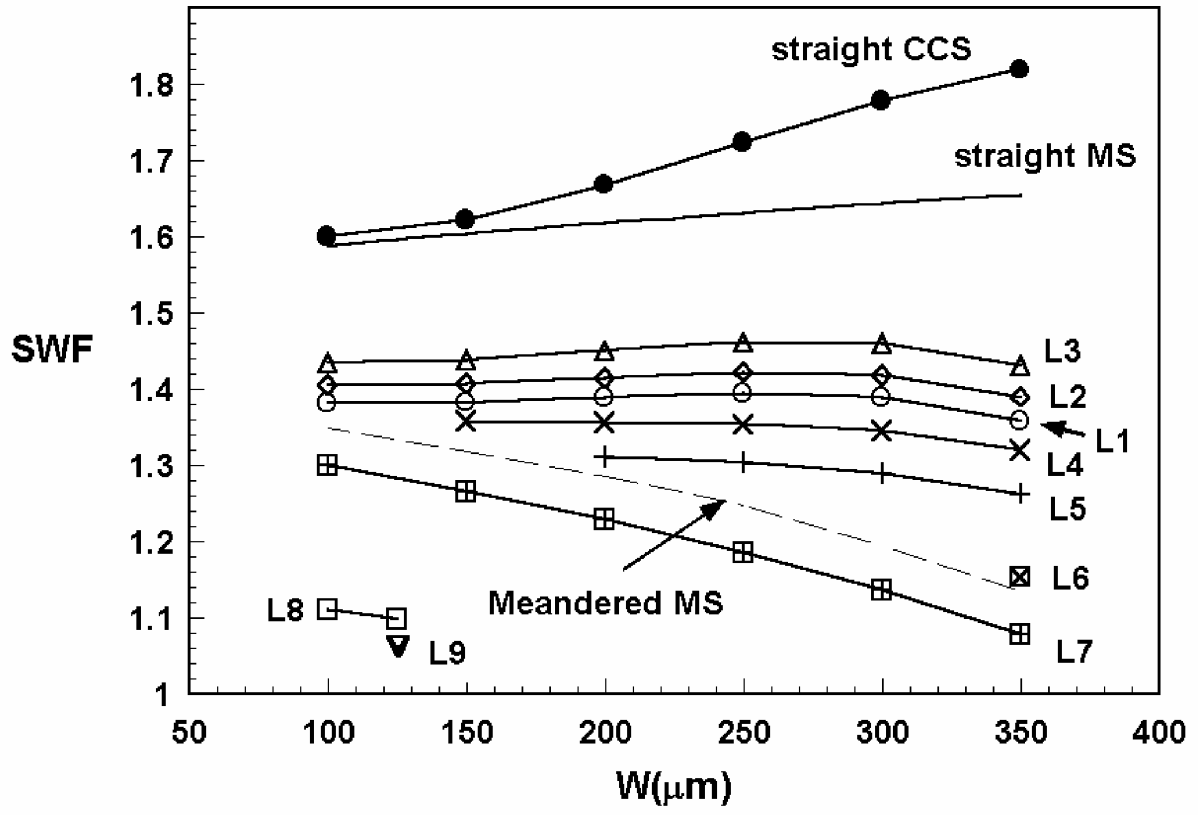

(b) The SWF vs. W

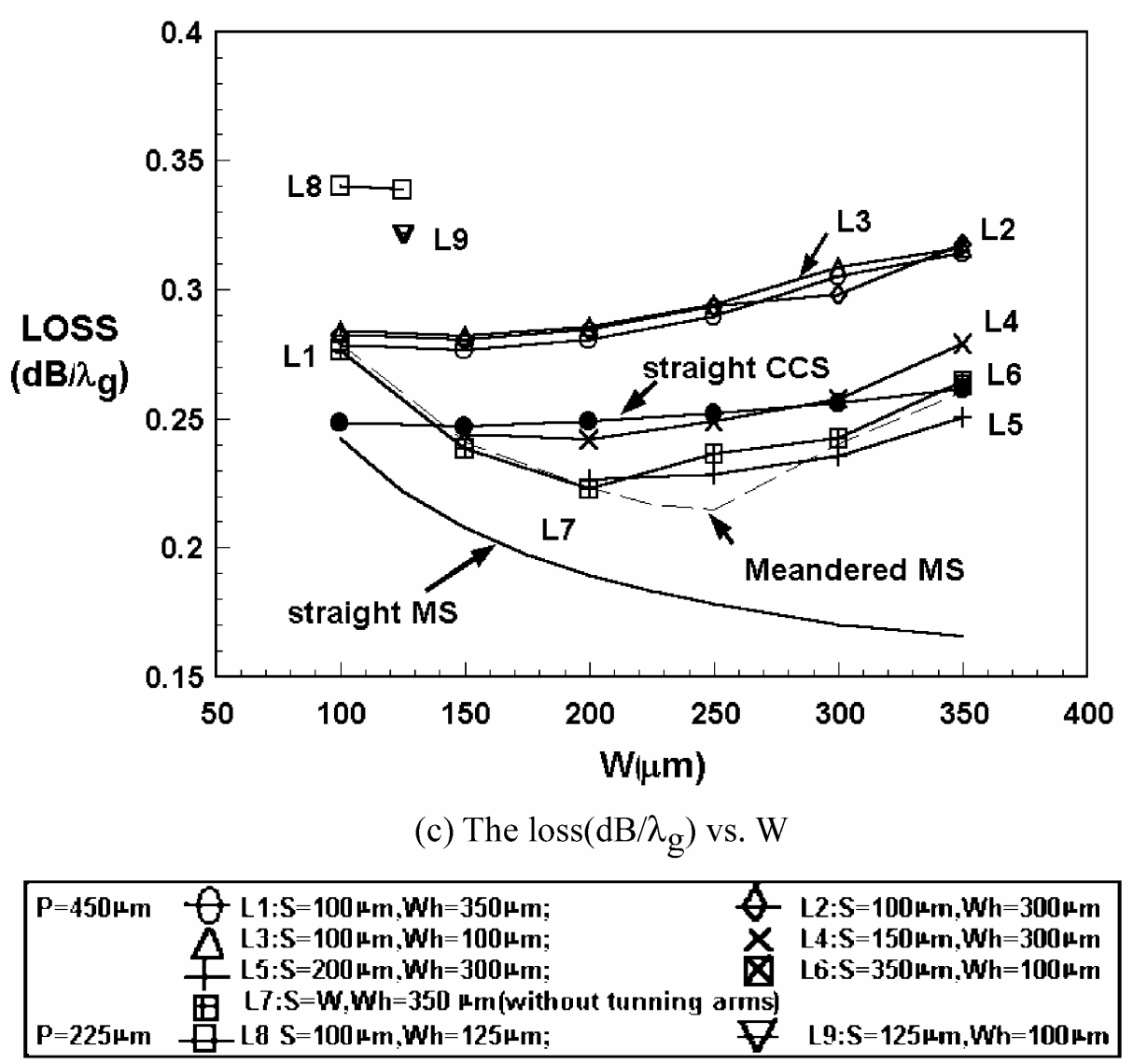

(c) The loss(dB/λ_g) vs. W

Fig. 3.5. Comparison of guiding properties. (a) Re(Z_c), (b) SWF, and (c) loss per guided wavelength (decibels/λ_g), of the CCS TL and MS in both straight and meandered configurations (5×4 meander trace) versus patch width W (= W_x = W_y) given various widths (S) of the connecting arm and various sizes of etched ground planes W_h (= W_{hx} = W_{hy}) ; periodicity P = 450 and 225 μm at f_o = 5.4 GHz.

between the conventional MS and synthetic CCL TL are presented with emphasis on effects of meanderings on guiding characteristics.

Assuming that RO4003 substrate of thickness of 0.203 mm and relative dielectric constant of 3.38 is employed for the synthetic CCS TL design, we begin with a straight-line configuration for both conventional and synthetic MS investigations. Fig. 3.5(a) plots the real part of the deembedded characteristic impedances against the width (W) of MSs. The lower bound of the width W is 100 μm, reflecting the typical limit of the present PCB foundry design rules. The upper bound is set to 350 μm, allowing room for the design of a high-impedance synthetic CCS TL.

The characteristic impedance of a straight CCS TL, in the L1 cell form, is 9.43%, 28.75%, and 27.83% higher than that of a straight MS line at W = 100, 200, and 350 μm, respectively. For the particular case of the straight CCS TL, the width of connecting arm S and the dimension of a square ground plane opening W_h are 100 and 350 μm, respectively. The combined result of alternating: 1) the MS and 2) the MS with the tuning septa produce the effective characteristic impedance, which are deembedded from the theoretical end-to-end two-port scattering parameters of the overall CCS TL, which is much greater than the conventional straight MS line.

The results of the second comparative study are also superimposed to the previous study, namely, the meandered MS and the meandered synthetic CCS TL following the same winding course. The plot located in the lowest level of Fig. 3.5(a) is the change of characteristic impedance of a meandered MS in the course of a 5×4 matrix against the width of the patch. Notice that the meandered arrangement of the MS significantly reduces the characteristic impedance by approximately 8.7 to 21.24% across the range of width variation from 100 to 350 μm in the particular case study. The corresponding meandered synthetic CCS line, marked by L1, shows the variation of Z_c from 106.4 to 72.8 Ω in contrast to the impedance variation from 103.4 to 50.3 Ω observed in the meandered MS. This particular case study clearly indicates that the synthetic CCS TL is less susceptible to meanderings than MS. Notice that periodicity (P) of 450 μm is assumed in this particular case study. When W = 350 μm, the minimum spacing between two meandered MSs (synthetic CCS TL) is only 100 μm, which is one-half of the substrate height, the adjacent lines in the meandered 5×4 matrix must couple strongly. Nevertheless, the CCS TL shows a stronger resistance to lowering the characteristic impedance by meanderings, thus, the slope of the L_1 curve is much flatter than that of the black dashed line of the meandered MS.

The third comparative study compares the variations characteristic

impedances within the meandered CCS TLs by varying the ground-plane openings from W_h = 350 μm to W_h = 100 μm while maintaining the same width of the connecting arm at S = 100 μm. As expected, reducing the size of the ground-plane opening or, equivalently narrowing the gap of the tuning septum, the characteristic impedance should be lower [52]. The results, marked by L1, L2, and L3 with symbols in hollow circle (0), hollow rhombus (◊), and triangle, successively decrease in values at an approximately equal increment as W varies. The lowest Z_c of these three plots occur for L3 at W = 350 μm, implying that a small perturbation in the ground plane by etching a square hole of 100 μm × 100 μm can still result in a much higher Z_c of 65.3 Ω, 30% greater than that of a meandered MS. In the third comparative study, the L1 curve (with W_h = 350 μm) shows the highest value in Z_c.

The fourth comparative study investigates the effect of S (width of the connecting arm of the CCS cell) on Z_c for periodicity P equal to 450 μm and a ground-plane square hole opening of 300μm × 300μm. This is equivalent to saying that, beginning with the L2 curve (connected by rhombus symbols), we increase the value of S from 100 μm through 150 μm, to 200μm. The results are represented by L2, L4, and L5, respectively. To our expectation again, an increase in S results in a wider MS section of the CCS TL, therefore, lowering Z_c. Consequently, L5 shows the lowest Z_c in this comparative study. L2, L4, and

L5 stretch out to the right for W = 100, 150, and 200 μm, respectively. Notice that the left-hand-side starting points of L2, L4, and L5 form an asymptote that is very close to the plot of the meandered MS. Such observation indicates that the CCS TL with S = W and W_h = 300 μm has similar Z_c to that of the meandered MS, implying that W_h is not big enough for making an impact on guiding properties.

If we decrease the value of W_h further to 100 μm, with anticipation that the meandered CCS TL behaves like a meandered MS, the results are plotted as a single point L6 for S = 350 μm, clearly showing that L6 is on the same Z_c plot of the meandered MS. If we increase the value of W_h from 300 to 350 μm by merely 50 μm and keep S = W, the resultant plot L7 shifts upwardly from the asymptote or the Z_c plot of the meandered MS, implying that the size of ground-plane opening is large enough to make a noticeable effect on guiding characteristics.

The last and sixth comparative study is based on a smaller cell size of P equal to 225 μm. Limited by the PCB design rules, the permissible tuning range is much smaller. Assuming that W_h = 125 μm, the results are shown in plot L8 for W between 100-125 μm. When compared to plots L1, L2, and L3 that incorporate design rules of S = 100 μm and P = 450 μm, one observes that use

of a smaller cell may pay the penalty for smaller Z_c. At W = 100 μm, the highest value of Z_c of L8 is 96.3Ω, considerably smaller than those that appear in L7, L1, and L2.

Fig. 3.5(b) plots the SWF of all case studies reported in Fig. 3.5(a) against the variation of width (W) in MS or CCS TL. One immediately recognizes that meanderings of TLs also cause a significant reduction in the SWF. For the particular MS, the effect of meanderings on a slow-wave reduction can be as high as 15.02% for W = 100 μm and 31.45% for W = 350 μm. Case studies of L1-L5, which exhibit higher resilience to the effect of meandering on a change of Z_c, also display relatively flat curves. Comparing cases L1-L3, increasing W_h (the size of the opening in the ground plane) results in a decrease in the SWF and an increase in Z_c. Examining L4 and L5, an increase of S (the width of connecting arms) reduces Z_c and SWF simultaneously. The mechanism by which the SWF decreases by increasing S reduces the SWF and mainly involves a fall in the equivalent inductive component of the stepped MS [55]. The meandered CCS TL of equal S and W, however, displays a constant downward shift from the plot for the meandered MS, reflecting the fact that the ground-plane openings actually decrease the SWF, as in the case studies of L1-L3 have demonstrated. When P = 225 μm, half of the previous case studies of L1-L7, the SWF is near 1.1 or below, as observed in L8 and L9. The reduction in cell size (periodicity) P in this particular case study adversely

affects the SWF of the meandered CCS TL. Care should be exercised as to notdeteriorate the SWF below the lower bound limit of the meandered MS by properly designing a correct configuration of the CCS TL.

Fig. 3.5(c) reports the attenuation constant of the various TL designs in units of losses in decibels per guided wavelength (dB/λ_g). Since the SWFs of the meandered MS and CCS TL are lower than the straight MS (or straight CCS TL), one may speculate that the attenuation constant in decibels per guiding wavelength should be highest for L8 and L9, followed by L7, L5, L4, L1, L2, L3, etc., as observed in Fig. 3.5(b). This is, however, not the case of simply reversing the order of Fig. 3.5(b). Fig 3.5(c) shows that the straight MS line has the lowest value in loss for the entire range of W of interest. The meandered MS, which shows higher attenuation as expected, appears approximately having the lower bound attenuation constants to all meandered CCS TLs under investigation. Of more interest is the fact that the lowest attenuation constants of all case studies L1-L6 form an asymptote that is nearly the replica of that for the meandered MS. All case studies reported in Fig. 3.5(c) demonstrate that the attenuation constants are generally less than 0.35 dB per guided wavelength, which is a practical value for most distributed microwave-circuit designs.

3.2.3 Dispersion Characteristics of 2-D TLs

The dispersion characteristics of meandered TLs should be investigated before completing the comprehensive studies of the synthetic TLs. In Fig. 3.5, all results are focused on a single frequency at 5.4 GHz. This section pays attention to a specific design of the CCS TL using S as a control parameter for fine tuning the desired characteristic impedance to be used in Chapter 4, Section 4.1 for design of a rat-race hybrid.

The propagation characteristics, complex characteristic impedance, and the normalized attenuation in decibels per wavelength (dB/λ_g) versus frequency for the particular meandered CCS TL wandering in a 5 × 4 matrix with a ground opening of 300 μm × 300 μm are shown in Fig. 3.6(a)-(c), respectively. For comparative purpose, the results of the straight MS and the meandered MS are also included in Fig. 3.6. The structural dimensions of all case studies investigated here are listed in the caption of Fig. 3.6.

Fig. 3.6(a) shows normalized phase constant β/k_o versus frequency, which are nearly flat between 0.5-10 GHz for all case studies. The maximum variation of β/k_o is smaller than 0.065 in Fig. 3.6(a) for CCS TL with S = 100 μm. At 5.4 GHz, the corresponding values of β/k_o are 1.64, 1.42, 1.35, 1.29, and 1.20 for a

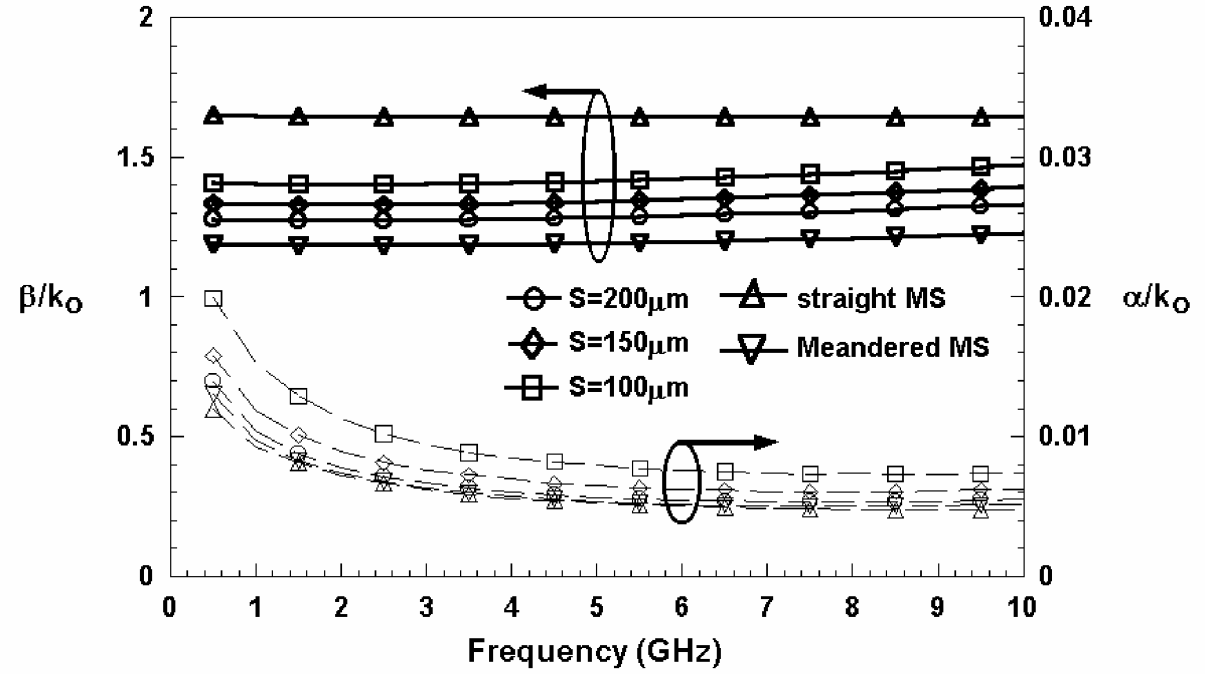

(a) The β/k_o, α/k_o vs. frequency

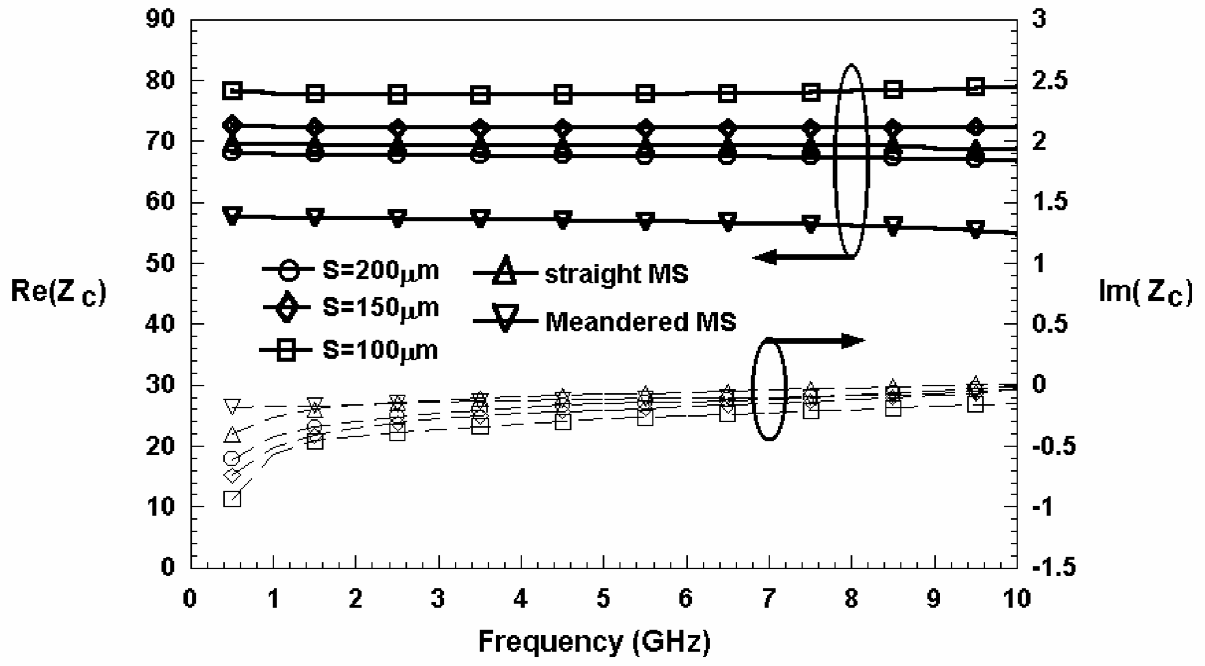

(b) The $Re(Z_c)$, $Im(Z_c)$ vs. frequency

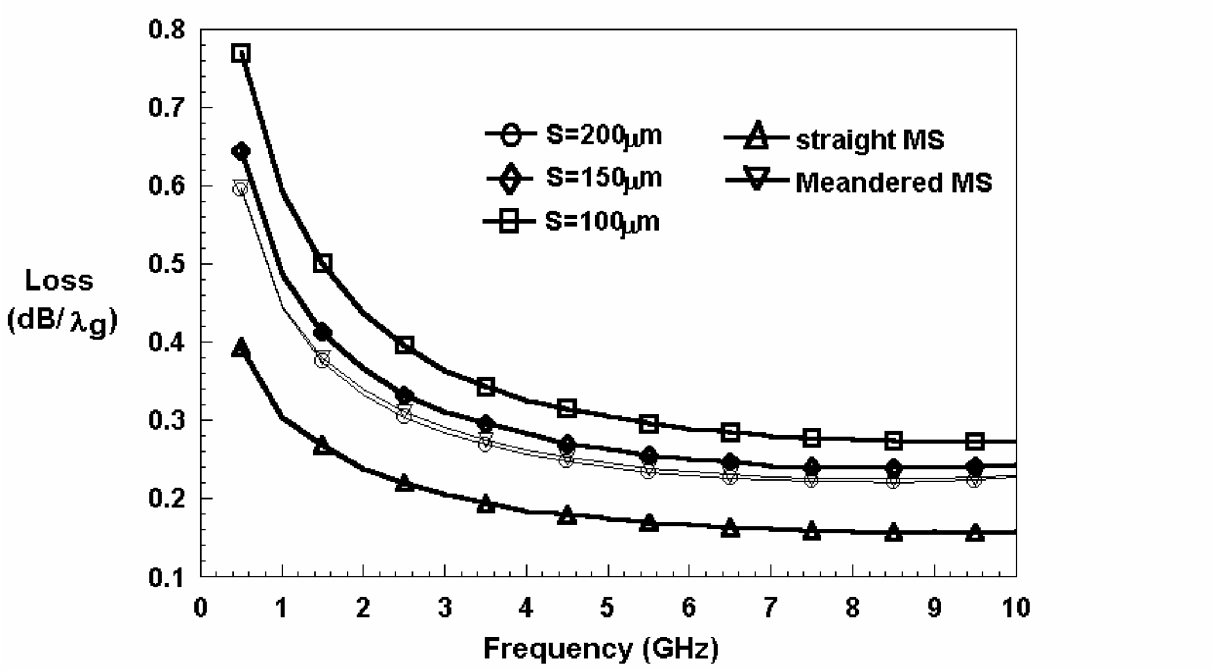

(c) The loss vs. frequency

Fig. 3.6. (a) Propagation characteristics (β/k_o, α/k_o), (b) complex characteristic impedance [Re(Z_c), Im(Z_c)], and (c) loss per guided wavelength (decibels/λ_g) versus frequency of the 2-D CCS TL (5×4 meander trace, the W_h = 300 μm) with various connecting arm widths S, and traditional MS and meandered MS with equal linewidths W (= 300 μm), total length L (= 9020 μm) and periodicity P (= 450 μm).

straight MS, meandered CCS TLs, and meandered MS, respectively. On the other hand, a decrease in the normalized attenuation constant α/k_o is noticeable between 0.5-3 GHz, and it flattens out from 3 to 10 GHz for all case studies. The maximum value of the α/k_o is approximately 0.02 and 0.007 at 0.5 and 10 GHz, respectively for the CCS TL with S = 100 μm. The values of α/k_o are 0.008, 0.006, 0.006, 0.005, and 0.005 for meandered CCS TLs with S = 100, 150, 200 μm, a meandered MS, and a straight MS at 5.4 GHz, respectively.

The left-hand-side axis of Fig. 3.6(b) plots the real part of Z_c (characteristic impedance) versus frequency, and is also showing that all cases are relatively flat. Maximum variation of $Re(Z_c)$ is only 3 Ω for the meandered MS case investigated at extreme frequencies. The value of $Re(Z_c)$ in descending order is approximately 78, 72, 70, 68, and 57 Ω for the meandered CCS TL with S = 100 and 150 μm, a straight MS, a meandered CCS TL with S = 200 μm, and a meandered MS, respectively, at f_o = 5.4 GHz. On the other hand, the imaginary part of Z_c slowly increases and flattens out as operating frequency increases. The imaginary part of Z_c is bounded in (-0.95, 0) Ω.

For purpose of clarity, we convert right-hand-side axis of Fig. 3.6(a) into loss in decibels per unit wavelength. The results are shown in Fig. 3.6(c). The maximum values of attenuation losses of the CCS TL with S = 100 μm is 0.77

and 0.27 dB/λ_g at f_o = 0.5 GHz and 10 GHz, respectively. Notice that the values of attenuation losses of CCS TLs with S = 150 and 200 μm are very close to those of the meandered MS.

The meandered CCS TL shows in all its aspects similar dispersion characteristics to those of a straight MS line. In practice, we treat the CCS TL like a quasi-TEM TL, although it is a 2-D guiding structure in nature.

3.2.4 Effect of Meandering Paths on the Compacted 2-D CCS TL

The sensitivity of guiding properties to the connecting form of the 2-D CCS TL in compacted microwave integrated circuits must be considered. The different meandering paths of the compacted 2-D CCS TL show as Fig. 3.7, which trace form be chosen will depend on your design requirements. Figure 3.8 (a)-(c) shows the propagation characteristics, complex characteristic impedance, and the normalized attenuation in decibels per wavelength (dB/λ_g) of the 2-D CCS TL (5 × 4) with different connecting form (trace pattern 1-3), respectively. Maintaining the same structural parameters, bottom surface pattern, and top surface pattern except for the connecting form of the unit cells of the 2-D CCS TL, the following three cases are simulated using the 5 × 4 CCS array, where S = 150 μm, $W_x = W_y$ = 300 μm, $W_{hx} = W_{hy}$ = 300 μm, P = 450 μm, and the total length L = 9020 μm.

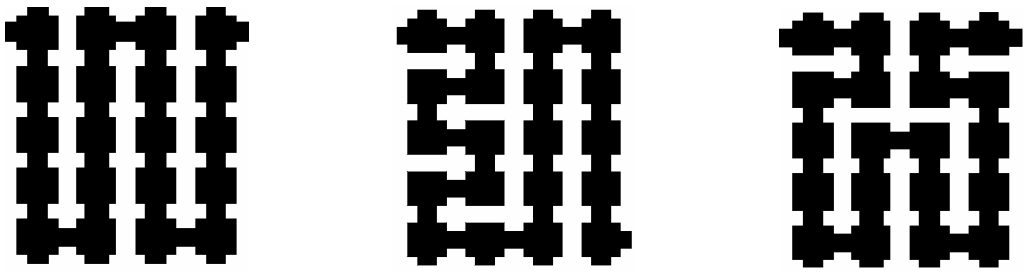

(a) (b) (c)

Fig. 3.7. The different meandering paths of the compacted 2-D CCS TL. (a) Trace pattern 1, (b) trace pattern 2, and (c) trace pattern 3.

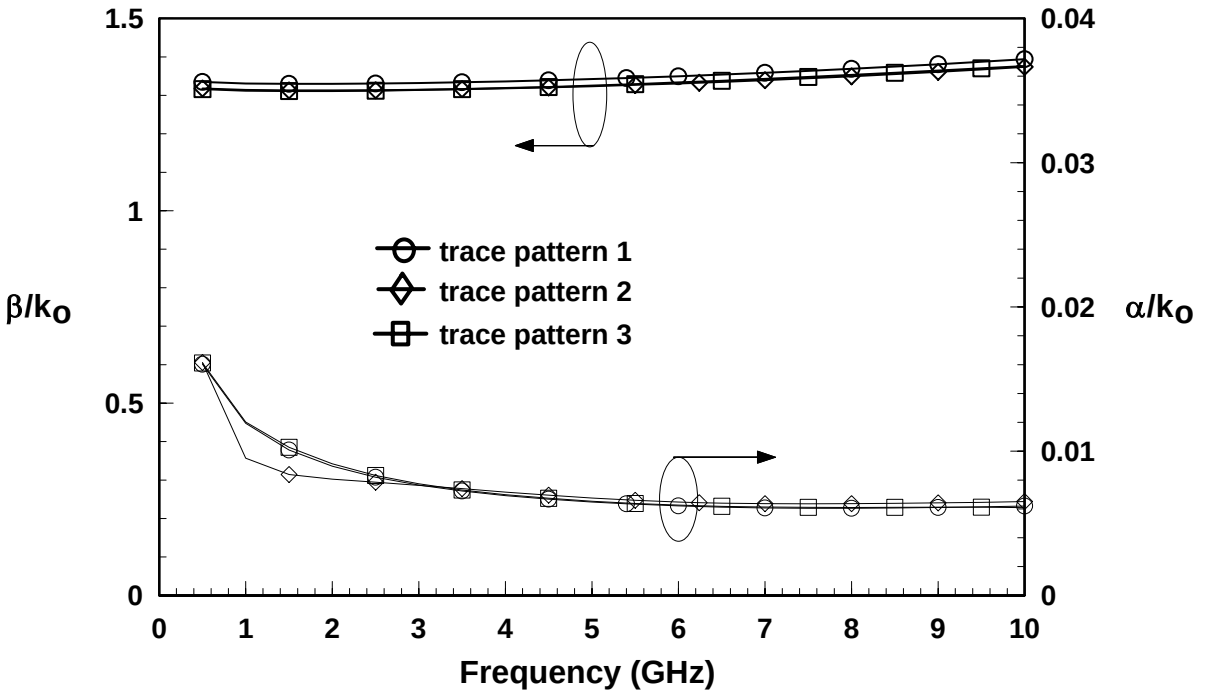

(a) The β / k_o, α / k_o vs. frequency

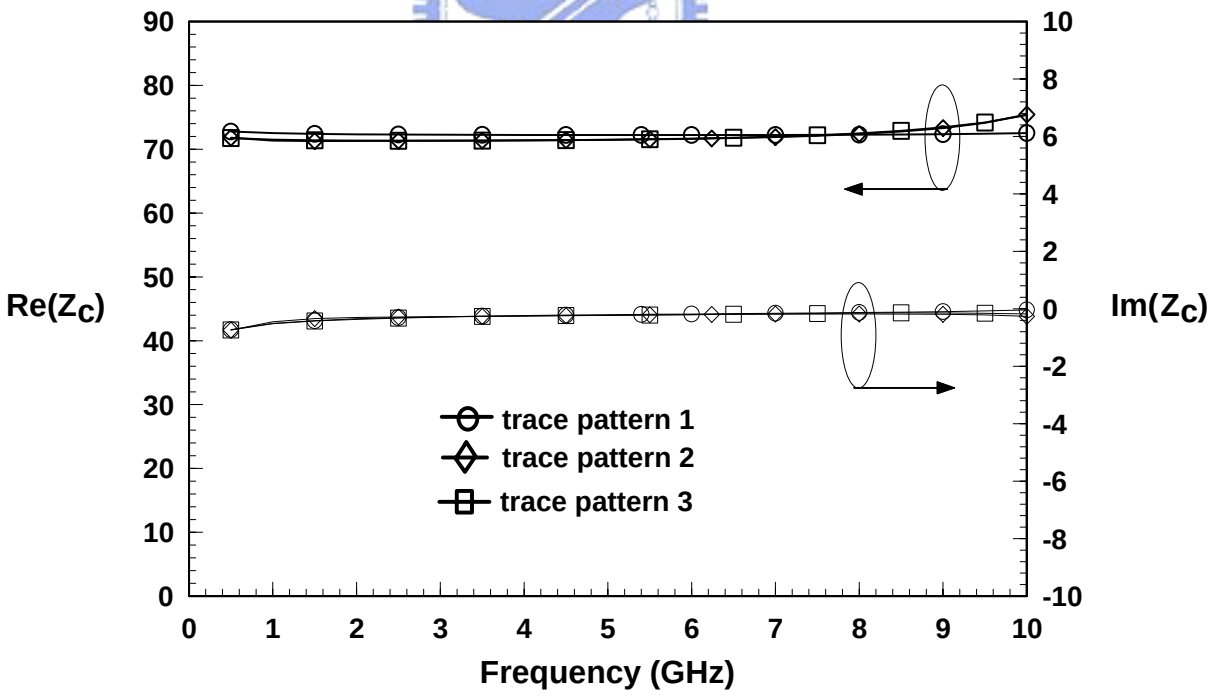

(b) The $Re(Z_c)$, $Im(Z_c)$ vs. frequency

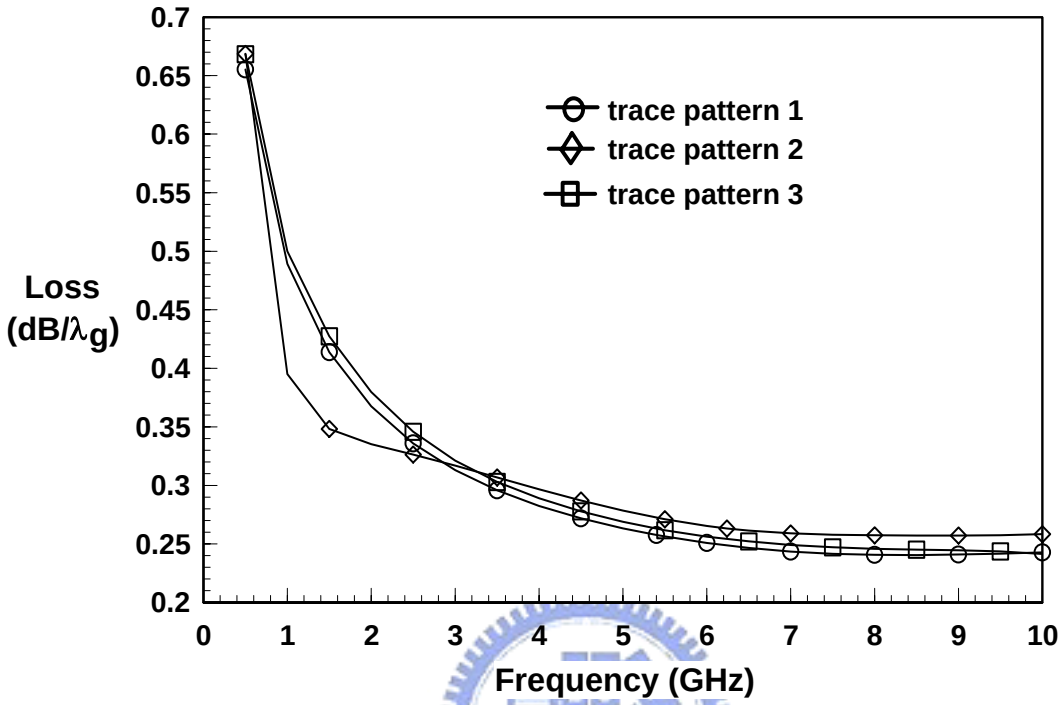

(c) The loss vs. frequency

Fig. 3.8. (a) Propagation characteristics (β/k_o, α/k_o), (b) complex characteristic impedance [Re(Z_c), Im(Z_c)], and (c) loss per guided wavelength (decibels/λ_g) versus frequency of the 70-Ω 2-D CCS TL (5 × 4) with different trace pattern 1, 2, and 3 as shown in Fig. 3.7, which the unit-cell structural parameters are same, the connecting arm width S = 150 μm, linewidth $W_x = W_y$ = 300 μm, hole width $W_{hx} = W_{hy}$ = 300 μm, periodicity P = 450 μm, and the total length L = 9020 μm.

The simulated guiding properties of these different trace pattern cases are almost identical, implying that the dispersion characteristics of the 2-D CCS TL are nearly the same despite the connecting form of the CCS unit cells in the top surface, provided the total length of the 2-D CCS TL is unchanged. That the connecting form of the 2-D CCS TL does not significantly alter the propagation characteristics and characteristic impedance is favorable for practical applications. Note also that the normalized attenuation constant and attenuation in decibels per guided wavelength are smaller for the case of trace pattern 2, which is not symmetry for the input and output (I/O) ports, in the lower frequency band, 0.5 - 2.5 GHz. For all cases, the magnitude of imaginary part of characteristic impedance $|\mathrm{Im}(Z_c)|$ is increased as frequency increasing, about 0-0.74 Ω at 0.5 - 10 GHz, it is obviously smaller than the real part values $|\mathrm{Re}(Z_c)|$, about 72 - 75 Ω at 0.5 - 10 GHz.

In the next Chapter, the trace pattern 1 and 3 of the 2-D CCS TL (5 × 4) with symmetrical I/O ports as showing in Fig. 3.7, will be chosen to design a compacted CCS rat-race hybrid.